INTERNATIONAL JOURNAL OF GEOMAGNETISM AND AERONOMY
VOL. 3, NO. 3, PAGES 217–228, FEBRUARY 2003

Variations in the rigidity spectrum and anisotropy of cosmic rays at the period of Forbush effect on 12–25 July 1982

V. M. Dvornikov and V. E. Sdobnov

Institute of Solar-Terrestrial Physics, Irkutsk, Russia

Abstract. Ground-based cosmic-ray (CR) observational data from a worldwide network of stations were used to investigate the variation of the CR distribution function and the changes in geomagnetic cutoff rigidities during the Forbush effect in July 1982. The data from 42 neutron monitors were employed in this study. The analysis was made by the method of spectrographic global survey. Using the worldwide network of stations as a single multichannel instrument, the method makes it possible to determine the parameters of the rigidity spectrum of CR variation and anisotropy in interplanetary space, as well as the changes of the planetary system of geomagnetic cutoff rigidities for every hour of observation. It is shown that at some instances a high degree of anisotropy is observed (the amplitude of the fundamental and second spherical harmonics is ∼10%–25% and ∼5%, respectively). A bidirectional anisotropy, which is characterized by a deficiency of particles with large pitch angles, was observed after the passage of regions with an increased interplanetary magnetic field (IMF) strength during the phase of solar wind velocity decrease when the Earth entered the IMF structure either with the field orientation normal to Parker's spiral or with the field polarity opposite with respect to the background polarity. Maximum values of the fundamental spherical harmonic amplitudes are observed in the phase of CR intensity decrease. The phase of the fundamental harmonic is orthogonal to the IMF vector. The variations have a very hard spectrum, and the spectral index is ∼0.4–0.5 in the main phase of the Forbush effect. A modulation mechanism is suggested, which permits the results to be explained.

1. Introduction

The problem of determining variations of the cosmic-ray CR distribution function outside the confines of the magnetosphere from ground-based observations presents considerable difficulty, and to solve it requires physically adequate assumptions about the form of the distribution function. All techniques available to date [*Baisultanova et al.,* 1987, 1991; *Dvornikov et al.,* 1983; *Krymskiy et al.,* 1966; *Nagashima,* 1971; *Shea and Smart,* 1982] take advantage of the assumptions either about the isotropic character of the CR distribution function or about the total separation of angular and energy variables, or about the separation of these variables for each spherical harmonic by expanding the distribution function in terms of spherical harmonics. In addition, the form of the rigidity dependence of the anisotropy is considered independent of time and is specified on the basis of some model for the propagation of particles in interplanetary space. This paper uses the technique (the method of spectrographic global survey (SGS)), the description of which is given in the section 2.

Using this technique, we investigate a giant Forbush decrease of 13–25 July 1982, characterized by significant CR modulation amplitudes ($\sim -20\%$ at the polar stations)

Paper number GAI01375.
CCC: 1524–4423/2001/0303–0375$18.00

The online version of this paper was published 25 November 2001.
URL: http://ijga.agu.org/v03/gai01375/gai01375.htm
Print companion issued February 2003.

and accompanied by geomagnetic disturbances with $Dst \sim -300$ nT.

2. Analysis Technique and Data

Our method is based on the assumption that the anisotropy in the CR distribution along the directions of the arrival is attributed to a dependence of their intensity on the pitch angle in the interplanetary magnetic field (IMF) and to a density gradient at the Larmor radius of particles.

In line with this assumption we will choose two orthogonal axes, one directed parallel (or antiparallel) to the IMF vector and the other directed to the vector $\mathbf{B}\times\boldsymbol{\nabla}n_\perp$, where $\mathbf{B}$ is the IMF vector and $\boldsymbol{\nabla}n_\perp$ is the CR density gradient component transverse with respect to $\mathbf{B}$. We now introduce a geocentric ecliptic coordinate system with the sunward directed axis OX. The angle between the particle velocity vector $\mathbf{V}$ and $\mathbf{B}$ (pitch angle) can then be defined by the expression

$$\cos\Theta = \mu = \sin\lambda\sin\lambda_0 + \cos\lambda\cos\lambda_0\cos(\Psi - \Psi_0) \quad (1)$$

and the angle between $\mathbf{V}$ and $\mathbf{B}\times\boldsymbol{\nabla}n_\perp$ is represented by

$$\cos\Phi = \nu = \sin\lambda\sin\xi_0 + \cos\lambda\cos\xi_0\cos(\Psi - \phi_0) \quad (2)$$

Here the angles Ψ_0 and λ_0 characterize the orientation of the first axis, and ϕ_0 and ξ_0 stand for the orientation of the second axis in our chosen coordinate system. The direction of motion of a particle is determined by the angles Ψ and λ.

In this case, from the orthogonality condition for the chosen axes, the angle ξ_0 can be expressed in terms of the angles Ψ_0, λ_0, and ϕ_0,

$$\xi_0 = \arctan\left[-(\cos\Psi_0\cos\phi_0 + \sin\Psi_0\sin\phi_0)\cos\lambda_0\right] \quad (3)$$

The CR intensity variation amplitudes observed on the ground may be represented by an expression of form [*Dorman,* 1957]

$$\frac{\delta I_c^i}{I_c^i}(h_l) = -\delta R_c W_c(R_c, h_c)\left[1 + \frac{\Delta J}{J}(R_c)\right] + \int_0^{2\pi}\int_0^{\pi/2}\int_{R_c}^{\infty}\frac{\delta J}{J}(R, \Psi(\alpha,\beta), \lambda(\alpha,\beta)) \times W_c^i(R,\alpha,\beta,h_l)\,\sin\beta\,d\beta\,d\alpha\,dR \quad (4)$$

Here $\delta I_c^i/I_c^i(h_l i)$ stands for variation amplitudes of an integral flux of secondary particles of sort i (with respect to a certain background level I_c^i) observed at a geographical site c at level h_l in the Earth's atmosphere; α and β are the azimuthal and zenith angles of arrival of primary particles at the atmospheric boundary; R_c is effective rigidity of geomagnetic cutoff; $W_c^i(R,\alpha,\beta,h_l)$ is the coupling function between primary and secondary CR variations; and $\Psi_c(R,\alpha,\beta)$ and $\lambda_c(R,\alpha,\beta)$ are the asymptotic angles of arrival of particles; $\delta R_c(R_c)$ is a probable variation in geomagnetic cutoff rigidity R_c. According to *Dvornikov and Sdobnov* [1991], dependence of δR_c on R_c was approximated by relations of the form

$$\delta R_c(R_c) = (b_1 R_c + b_2 R_c^2)\exp(-\sqrt{R_c})$$

$$(\delta J/J)(R_c) = \sum_{k=1}^{M_0} a_{0k} R_c^{-k}$$

are the amplitudes of CR global intensity variations at the threshold rigidity R_c.

Next, it will be assumed that flux density variations of primary CR particles are represented by

$$\frac{\delta J}{J}(R,\Psi,\lambda) = \sum_{k=0}^{M_0} a_{0k}R^{-k} + \sum_{n=1}^{N}\sum_{k=1}^{M_n}\left[\left(c_{nk}R^{-k}\right)P_n(\mu) + \left(d_{nk}R^{-k}\right)P_n(\nu)\right] \quad (5)$$

where $P_n(\mu)$ and $P_n(\nu)$ are the Legendre polynomials.

As follows from (5), the CR angular distribution are represented by two axially symmetric (with respect to the corresponding axis) anisotropy components, each of which has its own rigidity dependence. Rigidity spectra of the anisotropic component and of two anisotropy components are approximated rows from the inverse degree of rigidity.

In the solar-ecliptic coordinate system, expression (5) will be of the form

$$\frac{\delta J}{J}(R,\Psi,\lambda) = \sum_{k=1}^{M_0} a_{0k}R^{-k} + \sum_{n=1}^{N}\sum_{m=0}^{M_n}\left[a_n^m(R)\cos(m\Psi) + b_n^m(R)\sin(m\Psi)\right]P_n^m(\sin\lambda) \quad (6)$$

where

$$a_n^0(R) = \left(\sum_{k=1}^{M_n} c_{nk}R^{-k}\right)P_n(\sin\lambda_0) + \left(\sum_{k=1}^{M_n} d_{nk}R^{-k}\right)P_n(\sin\xi_0)$$

$$a_n^m(R) = \frac{2(n-m)!}{(n+m)!}\left[\left(\sum_{k=1}^{M_n} c_{nk}R^{-k}\right)\times P_n^m(\sin\lambda_0)\cos m\Psi_0\right.$$

$$+\left(\sum_{k=1}^{M_n} d_{nk}R^{-k}\right) P_n^m(\sin\xi_0)\cos m\phi_0\Bigg] \quad (7)$$

$$b_n^m(R) = \frac{2(n-m)!}{(n+m)!}$$

$$\times\Bigg[\left(\sum_{k=1}^{M_n} c_{nk}R^{-k}\right) P_n^m(\sin\lambda_0)\sin m\Psi_0$$

$$+\left(\sum_{k=1}^{M_n} d_{nk}R^{-k}\right) P_n^m(\sin\xi_0)\sin m\phi_0\Bigg]$$

Upon substituting expression (6) into the equation of variations (4), we obtain the following system of nonlinear algebraic equations:

$$\frac{\delta I_c^i}{I_c^i}(h_i) = (b_1R_c + b_2R_c^2)\exp(-\sqrt{R_c})W_c(R_c,h_l)$$

$$+\int_0^{2\pi}\int_0^{\pi/2}\int_{R_c}^{\infty}\Big\{\sum_{k=1}^{M_0} a_{0k}R^{-k}$$

$$+\sum_{n=1}^{N}\sum_{m=0}^{n}[a_n^m(R)\cos m\Psi_s(R,\alpha,\beta)$$

$$+b_n^m(R)\sin m\Psi_c(R,\alpha,\beta)]P_n^m(\sin\lambda(R,\alpha,\beta))\Big\}$$

$$\times W_c^i(R,\alpha,\beta,h_i)\sin\beta d\beta d\alpha dR \quad (8)$$

If in (6) and (7) we confine ourselves to two spherical harmonics to describe each of the anisotropy components ($N = 2$) and if we set $M_0 = 3$ and $M_1 = M_2 = 2$, then the problem is reduced to a search for the following unknown parameters: b_1, b_2, a_{01}, a_{02}, a_{03}, c_{11}, c_{12}, c_{21}, c_{22}, d_{11}, d_{12}, which characterize variations of geomagnetic cutoff rigidity R_c, differential rigidity variation spectra of the isotropic component and two components of the first and second harmonics of the CR angular distribution; Ψ_0, λ_0, ξ_0, and ϕ_0 determine the orientation of the chosen symmetry axes.

To solve the above formulated problem, the world stations network and detector systems there must ensure redundancy and linear independence of the system of equations (8). In solving the problem the angles Ψ_0, λ_0, and ϕ_0 are subjected to the Monte Carlo method, and the angle ξ_0 is inferred from formula (3). Upon substituting values of the "played" angles into system (8), we obtain a system of linear equations that is solved by the least squares technique.

Values obtained for the roots of the system of equations (8) are used to calculate the amplitude $A_1(R)$ and the phase $\Psi_1(R)$, $\lambda_1(R)$ of the first spherical harmonic for particles with rigidity R by the formulas

$$A_1(R) = \left\{\left[a_1^0(R)\right]^2 + \left[a_1^1(R)\right]^2 + \left[b_1^1(R)\right]^2\right\}^{0.5}$$

$$\Psi_1(R) = \arctan\frac{b_1^1(R)}{a_1^1(R)} \quad (9)$$

$$\lambda_1(R) = \arcsin\frac{a_1^0(R)}{A_1(R)}$$

as well as amplitudes and phases of the zonal ($m = 0$), tesseral ($m \neq n$), and sectorial ($m = n$) components of the second and the third harmonic:

$$A_n^0(R) = a_n^0(R)$$

$$A_n^m(R) = P_n^m(\sin\lambda)\sqrt{[a_n^m(R)]^2 + [b_n^m(R)]^2} \quad (10)$$

$$\Psi_n^m(R) = \arctan\frac{b_n^m(R)}{a_n^m(R)}$$

where $a_n^m(R)$ and $b_n^m(R)$ are defined by expression (7).

As follows from (9) and (10), unlike all existing techniques, in the proposed method the form of rigidity dependencies of the anisotropy is determined for each instant of time, while phases of the first, tesseral, and sectorial components of the second harmonic depend on particle rigidity. When developing the method, we used more than 10 representations of the CR distribution function that reflect different models for the propagation of particles in the heliosphere, but the best agreement with ground-based and satellite measurements in analyzing the phenomenon under investigation was obtained for a distribution function of the form (5). Calculations were based on coupling functions between primary and secondary CR reported [*Lockwood and Webber*, 1967; *Webber*, 1962; *Webber and Quenby*, 1959] (corrected for an 11-year variation) and on asymptotic angles obtained through trajectory calculations [*McCracken et al.,* 1965; *Shea et al.,* 1965] as well as formulas for transition to the chosen coordinate system [*Dorman,* 1975].

The analysis used data from the worldwide network of neutron monitor stations corrected for pressure and averaged for 2-hour time intervals [*World Data Center C2*]. Modulation amplitudes were measured from the background level of 9 July. The data were from 42 neutron monitors, which are listed in Table 1.

3. Analysis Results

Figure 1 presents the data of space-based in situ measurements of the solar wind (SW) velocity, the IMF modulus in nT, the angles Ψ and λ, which characterize the orientation of the IMF vector in interplanetary space for the period under consideration, the time profiles of variations in global CR intensity with the rigidity of 4 and 20 GV, the modulus of

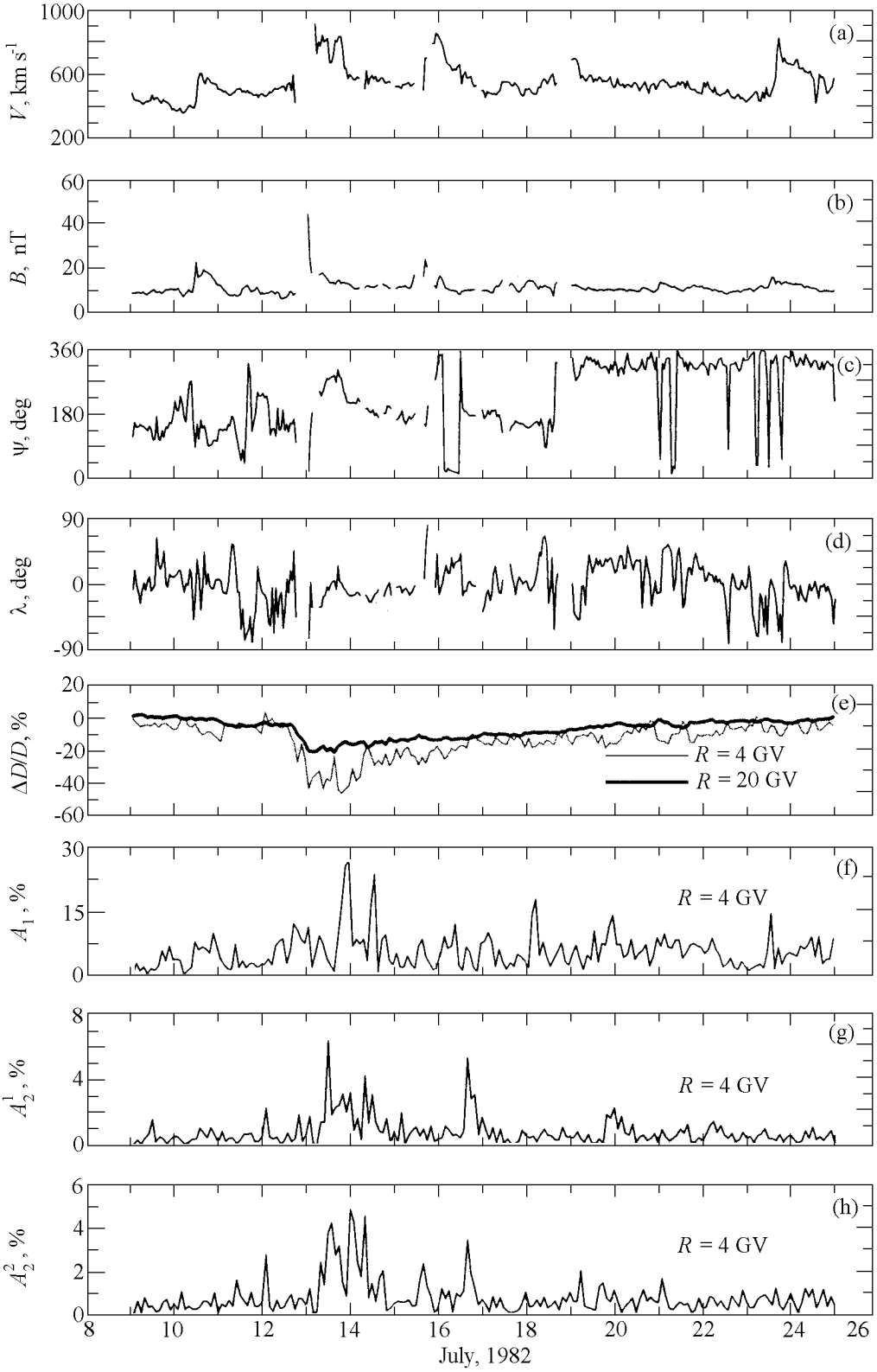

Figure 1. Variations of (a) solar wind velocity, (b) IMF modulus, (c) azimuth angle ψ and (d) latitude angle λ, which characterize the IMF vector orientation in the heliocentric ecliptic reference frame, (e) variations in global intensity of CRs with $R_c = 4$ and 20 GV, (f) amplitudes of the modulus of the first spherical harmonic A_1 for the particles with $R_c = 4$ GV, (g) amplitudes of the tesseral component of the second harmonic A_2^1 for the particles with $R_c = 4$ GV, and (h) amplitudes of the sectoral component of the second harmonic A_2^2 for the particles with $R_c = 4$ GV.

Table 1. List of the Neutron Monitor Stations

	Station	Geographical Coordinates		Altitude, m	Cutoff Rigidity, GV
		Latitude, deg	Longitude, deg		
1	Alert	82.50 N	62.33 W	57	0.00
2	Alma-Ata A	43.25 N	76.92 E	806	6.61
3	Alma-Ata B	43.25 N	76.92 E	3340	6.61
4	Apatity	67.55 N	33.33 E	177	0.60
5	Climax	39.37 N	106.18 W	3400	2.97
6	Deep River	46.10 N	77.50 W	145	1.07
7	Dourbes	50.10 N	4.60 E	225	3.24
8	Durham	43.10 N	70.83 W	sl	1.57
9	Goose Bay	53.27 N	60.40 W	46	0.60
10	Hermanus	34.42 S	19.23 E	26	4.56
11	Huancayo	12.03 S	75.33 W	3400	13.01
12	Inuvik	68.35 N	133.72 W	21	0.16
13	Irkutsk	52.47 N	104.03 E	435	3.56
14	Irkutsk 2	52.28 N	104.02 E	2000	3.66
15	Irkutsk 3	52.28 N	104.02 E	3000	3.66
16	Jungfraujoch	46.55 N	7.98 E	3570	4.53
17	Kerguelen	49.35 S	70.27 E	33	1.19
18	Kiel	54.34 N	10.12 E	54	2.32
19	Kiev	50.72 N	30.30 E	120	3.48
20	Leeds	53.80 N	1.55 W	72	2.17
21	Lomnicky Stit	49.20 N	20.22 E	2634	4.00
22	Magadan	60.12 N	151.02 E	220	2.11
23	McMurdo	77.90 S	166.60 E	48	0.00
24	Morioka	39.70 N	141.13 E	131	10.05
25	Moscow	55.47 N	37.32 E	200	2.39
26	Mt. Norikura	36.11 N	137.55 E	2770	11.36
27	Mt. Washington	44.27 N	71.30 W	1900	1.38
28	Mt. Wellington	42.92 S	147.25 E	725	1.82
29	Newark	39.70 N	75.70 W	50	2.02
30	Oulu	65.06 N	25.47 E	sl	0.77
31	Potchefstroom	26.68 S	27.10 E	1351	6.97
32	Predigtstuhl	47.70 N	12.88 E	1614	4.29
33	Rome	41.90 N	12.52 E	60	6.24
34	Sanae	70.31 S	2.40 W	52	0.91
35	South Pole	90.00 S	0.00 E	2820	0.09
36	Sverdlovsk	56.43 N	60.57 E	300	2.29
37	Tashkent	41.33 N	69.62 E	565	7.47
38	Tbilisi	41.72 N	44.80 E	510	6.66
39	Terre Adelie	66.67 S	140.02 E	35	0.00
40	Tixie Bay	71.58 N	128.92 E	sl	0.45
41	Tokyo	35.75 N	139.72 E	20	11.50
42	Tsumeb	19.20 S	17.58 E	1240	9.29

the fundamental spherical harmonic and of the amplitude of the tesseral ($m \neq n$) and sectorial ($m = n$) components of the second harmonic. Figure 2 presents the variations in geomagnetic cutoff rigidity ΔR_c for $R_c = 4$ GV together with the *Dst* index, and the values of the standard deviations δ of the observed variation amplitudes from the calculated ones.

Figure 3 (left and right, respectively) shows the dependencies of variations in geomagnetic cutoff rigidity ΔR_c on the geomagnetic cutoff rigidity R_c obtained from the analysis, and the results of calculations of $\Delta R_c(R_c)$ [*Dorman and Tyasto*, 1965; *Treiman*, 1953] for the model of the magnetospheric current flowing in a westward direction along the parallels on a sphere with the force proportional to the latitude cosine [*Chapman*, 1937].

A maximum modulation amplitude for particles with $R =$ 4 and 20 GV was observed on 14 July to make up $\sim -40\%$ and $\sim -20\%$, respectively. The variations show a very hard spectrum (the spectral index of the variations $\gamma \approx 0.4$). A maximum anisotropy amplitude was observed at the period of a maximum modulation on 14 and 15 July with $A_1 \sim 25\%$, and A_{12} and $A_{22} \sim 5\%$ for particles with $R = 4$ GV.

The CR intensity distribution with $R = 4$ GV for the

times of observation of a maximum anisotropy is presented in the top panel of Figure 4. Numbers at the contours correspond to the CR intensity variation amplitudes as a percentage of the background level. The plus symbols designate the orientation of the IMF vector at the instants of time under consideration.

4. Discussion and Conclusions

As is evident from the results presented above, some instants of time of the period under investigation show a bidirectional anisotropy of a large amplitude in the angular distribution of particles, which suggests, on the one hand, the presence of structures like a magnetic trap and, on the other hand, the smallness of the diffusion coefficient in the momentum space. A combined analysis of the variations of the CR distribution function and the IMF data intimates that the bidirectional anisotropy, which is characterized by a deficiency of particles with large pitch angles, is observed after the passage of regions with an increased IMF strength when the Earth enters the IMF structures, either with the IMF orientation normal to the Parker spiral (beginning of 13 and 14–15 July) or with the opposite field polarity with respect to the background polarity (17 July). This suggests that during the period of the concerned event, loop-like structured magnetic field fluxes are transported away; while traveling away from the Sun, they drive out the background magnetic field by deforming it, especially at the leading edge, as shown in Figure 5.

CRs penetrate into the magnetic trap and escape it through centrifugal and gradient drifts of particles, and the increase in intensity is due to a change in the energy of CR as they travel in regular electromagnetic fields of the heliosphere.

The energy variation of particles $\Delta\mathcal{E}$ as they travel in the regular electromagnetic fields $\mathbf{E}$ and $\mathbf{B}$ can be estimated within the drift approximation by solving the system of equations [*Morozov and Soloviev*, 1963]

$$\frac{d\mathbf{r}}{dt} = v_{\parallel}\frac{\mathbf{B}}{B} + \frac{c}{B^2}\mathbf{E}\times\mathbf{B}$$

$$+\frac{mcv_{\parallel}^2}{eB^4}\mathbf{B}\times(\mathbf{B}\nabla)\mathbf{B} + \frac{mcv_{\perp}^2}{2eB^3}\mathbf{B}\times\nabla B \qquad (11)$$

$$\frac{d\mathcal{E}}{dt} = e\mathbf{E}\frac{d\mathbf{r}}{dt} + \frac{mv_{\perp}^2}{2B}\frac{\partial B}{\partial t} \qquad (12)$$

$$\frac{d\mathcal{J}_{\perp}}{dt} = 0 \qquad (13)$$

Here $v_{\parallel}$ and $v_{\perp}$ are the velocity components of a particle with the mass m and charge e parallel and perpendicular to the magnetic field $\mathbf{B}$; c is the velocity of light; $d\mathbf{r}/dt$ is the velocity of the center of the Larmor circle; $\mathcal{E} = (m_0c^2)/(1 - v^2/c^2)^{1/2}$ is the averaged energy; and $\mathcal{J}_{\perp} = (m^2v_{\perp}^2)/(m_0^2B)$ is the transverse adiabatic invariant.

The first term in equation (11) describes the motion of the particle along a magnetic field line, and the next three terms describe, the energy and the centrifugal and gradient drifts,

If $\mathrm{rot}\,\mathbf{E} = -(1/c)\times(\partial B)(\partial t) = 0$, and

$$\mathbf{E} = -\frac{1}{c}\mathbf{U}\times\mathbf{B} \qquad (14)$$

where $\mathbf{U}$ is the solar wind velocity, and the magnetic field, according to *Parker* [1963] have a radial and azimuthal component of the form

$$B(r) = B_r(r_0)\left(\frac{r_0}{r}\right)^2$$
$$B_{\varphi}(r,\lambda) = B_r(r,\lambda)\frac{\Omega r}{U}\sin\lambda \qquad (15)$$

where r is the radial distance from the Sun, λ is the heliolatitude, and Ω is the angular rotation velocity of the Sun; then by integrating (12), in view of (11), and (13)–(15) we obtain the expression for the energy variation of particles $\Delta\mathcal{E}$ in fields of the geometry under consideration [*Dvornikov and Matyukhin*, 1976; *Dvornikov et al.*, 1987]

$$\Delta\mathcal{E}_{pt} = \frac{e\Omega B_{r0}r_0^2}{c} \qquad (16)$$

Expression (16) shows how much the particle energy will decrease if it has travelled from the pole to the helioequator in a direction opposite to the electric field $\mathbf{E}$ (equation (14)).

The value of $\Delta\mathcal{E}$, with the IMF modulus ∼5 nT at the Earth's orbit, is ∼200 MeV and is independent either of the hardness of particles or of their pitch angle in the IMF because the electric field respectively. in (14) of a stationary, homogeneous SW is a potential one. Nor does this quantity depend on the SW velocity as the azimuthal IMF component in this case is inversely proportional to the SW velocity (15)

$$E_{\lambda} = \frac{1}{c}UB_{\varphi} = B_r(r,\lambda)\frac{\Omega r}{c} \qquad (17)$$

In the case where a loop-like structure of a high-speed solar wind is transported into interplanetary space, the situation reverses drastically. The electric field can have both a meridional, E_{λ}, and an azimuthal, E_{φ}, component. The strength of this field depends on the value of $(B_{\varphi}^2 + B_{\lambda}^2)^{1/2}$ and on the SW velocity and can exceed by more than an order of magnitude, the magnitude of the electric field caused by the IMF of a helical geometry. Accordingly, there will be an increase in energy losses ΔE_{pt}.

The variation in particle energy caused by the vortical component of the electric field (the second term on the right-hand side of equation (12)) is defined by the expression

$$\Delta\mathcal{E}_{\mathrm{rot}} = \mathcal{E} - \sqrt{\beta(\mathcal{E}^2 - \varepsilon_0^2) + \mathcal{E}_0^2} \qquad (18)$$

where $\beta \propto (B/B_0)$, B_0 and B are the strengths of the background magnetic field and of the variable field, respectively, and ε is the rest energy.

Besides, *Dvornikov and Sdobnov* [1997a, 1997b] conjectured that polarization electric fields exist in the heliosphere, which are produced at the propagation of accelerated particles in inhomogeneous fields of the heliosphere.

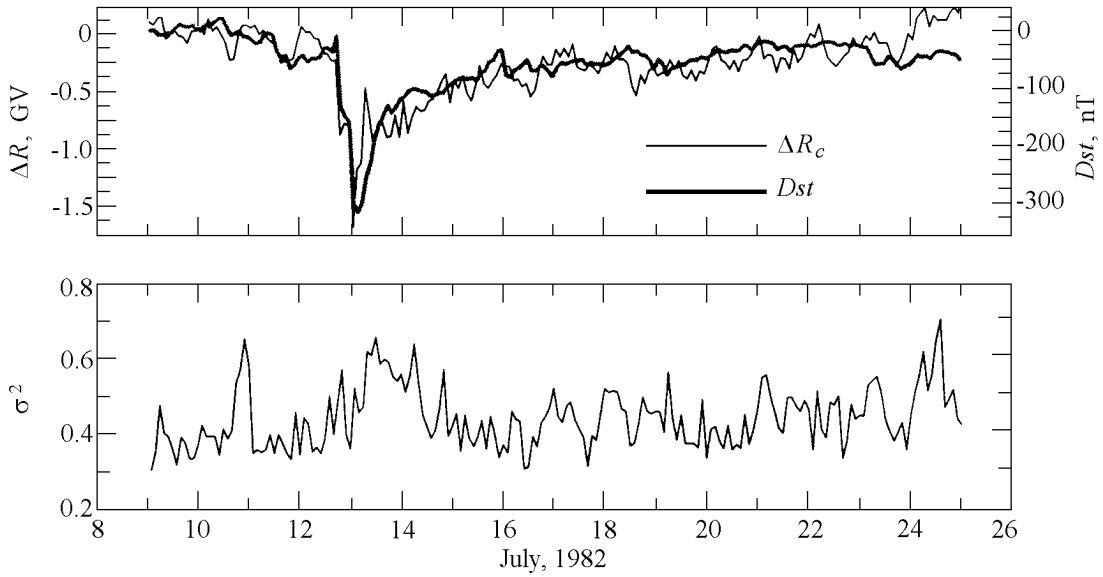

Figure 2. Variations in geomagnetic cutoff rigidity for $R_c = 4$ GV and in the *Dst* index. The bottom panel demonstrates the mean square deviations (δ) of the observed variation amplitudes from the calculated ones.

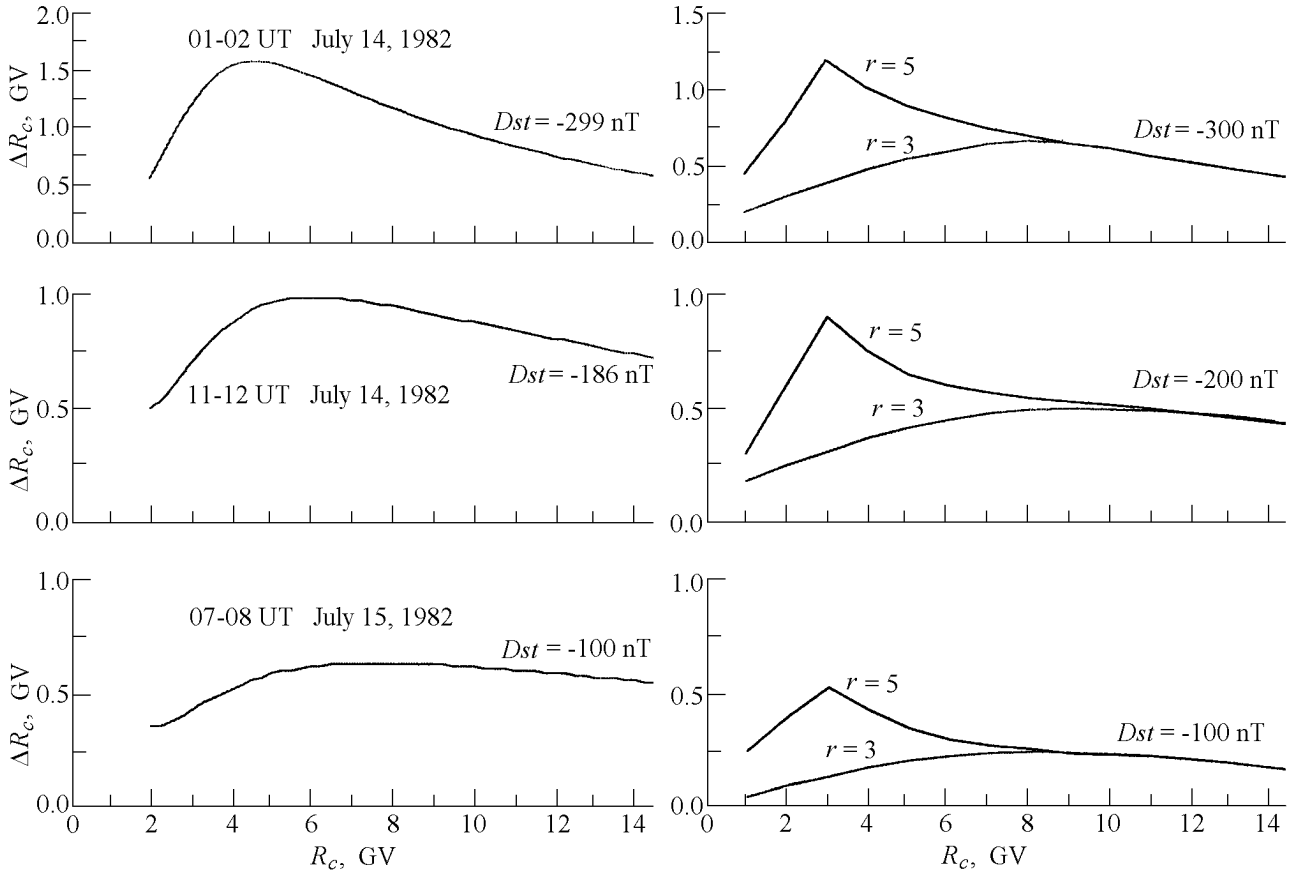

Figure 3. Variations in geomagnetic cutoff rigidity ΔR_c versus geomagnetic cutoff rigidity R_c for various time moments and for various *Dst* (left-hand panels). At the right-hand panels there are ΔR_c calculated by the model of the magnetospheric currents flowing westward along the parallels of the sphere and having values proportional to the cosine of the latitude. The numerals at the curves indicate the distance to the current shell in terms of the Earth's radii.

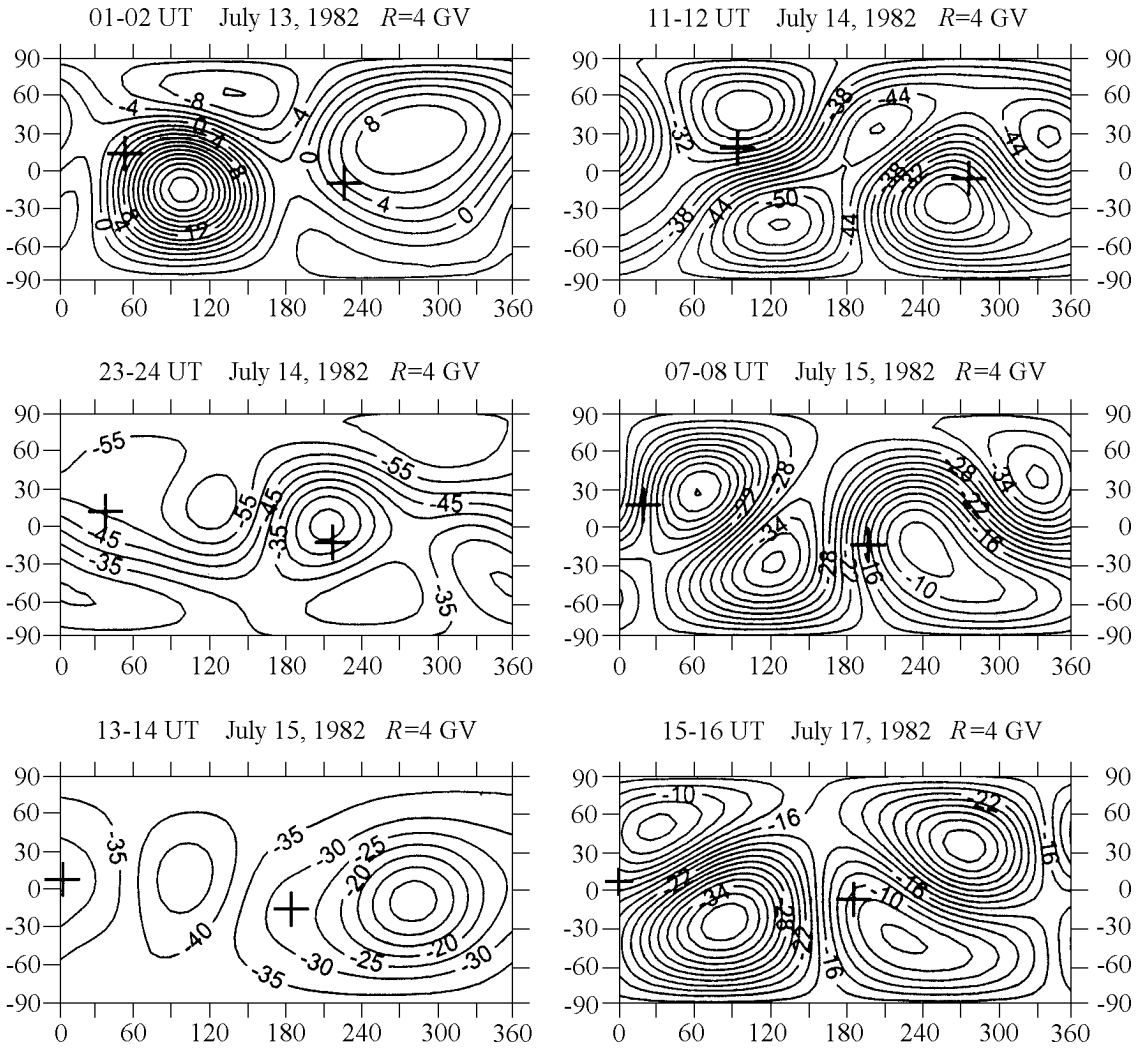

Figure 4. Relative intensity variations of the CRs with $R_c = 4$ GV versus asymptotic directions in the solar-ecliptic frame for different moments of time.

If the perpendicular (to the magnetic field) component of the polarization electric field $E_{\mathrm{pl}\perp} \sim (v/c)B$, and $E_{\mathrm{pl}\parallel} \ll (v/c)B$, then equation (11) becomes

$$\frac{d\mathbf{r}}{dt} = \mathbf{u} - \frac{mc}{eB^2}\left[\frac{\partial \mathbf{u}}{\partial t} + (\mathbf{u}\bigtriangledown)\,\mathbf{u}\cdot\mathbf{B}\right] + \frac{mcv_\perp^2}{2eB^3}\mathbf{B}\times\bigtriangledown B \qquad (19)$$

and the energy $\mathcal{E}$ in equation (12) is defined by the expression $\mathcal{E} = (m/2)\left(v_\parallel^2 + v_\perp^2 + v_E^2\right)$; $\mathbf{u} = v_\parallel(\mathbf{B}/B) + \mathbf{v}_E$; $\mathbf{v}_E = (c/B^2)\mathbf{E}\times\mathbf{B}$.

The second terms on the right-hand side of equation (19) is integrated as a drift under the action of the inertial force $m\left[(\partial\mathbf{u}/\partial t) + (\mathbf{u}\bigtriangledown)\mathbf{u}\right]$

In this case, the variation in particle energy under the action of the electric field $\mathbf{E}_{\mathrm{pl}}$, provided that $\mathbf{E}_{\mathrm{pl}}$ is a linear function of time, is represented as

$$\Delta\mathcal{E}_{\mathrm{pl}} = \mathcal{E}(1 - \exp(\alpha/2)) \qquad (20)$$

where $\alpha = E_{\mathrm{pl}}^2/B^2$.

Polarization electric fields can be produced in the case of large-particle density gradients and a strong inhomogeneity of the magnetic field. Large-particle density gradients can arise in coronal loop-like structures of magnetic field when the magnetic field strength of these structures increases with time. In this case, cosmic rays are drifting toward the axis of the current system, which forms a loop-like structure, and are accelerated by the betatron mechanism; that is, the energy accumulation process is taking place.

Once critical values of the current are attained, the current system can be disrupted, which is accompanied by an explosive process and hence by an enhancement of the magnetic field inhomogeneity, i.e., by the production of condi-

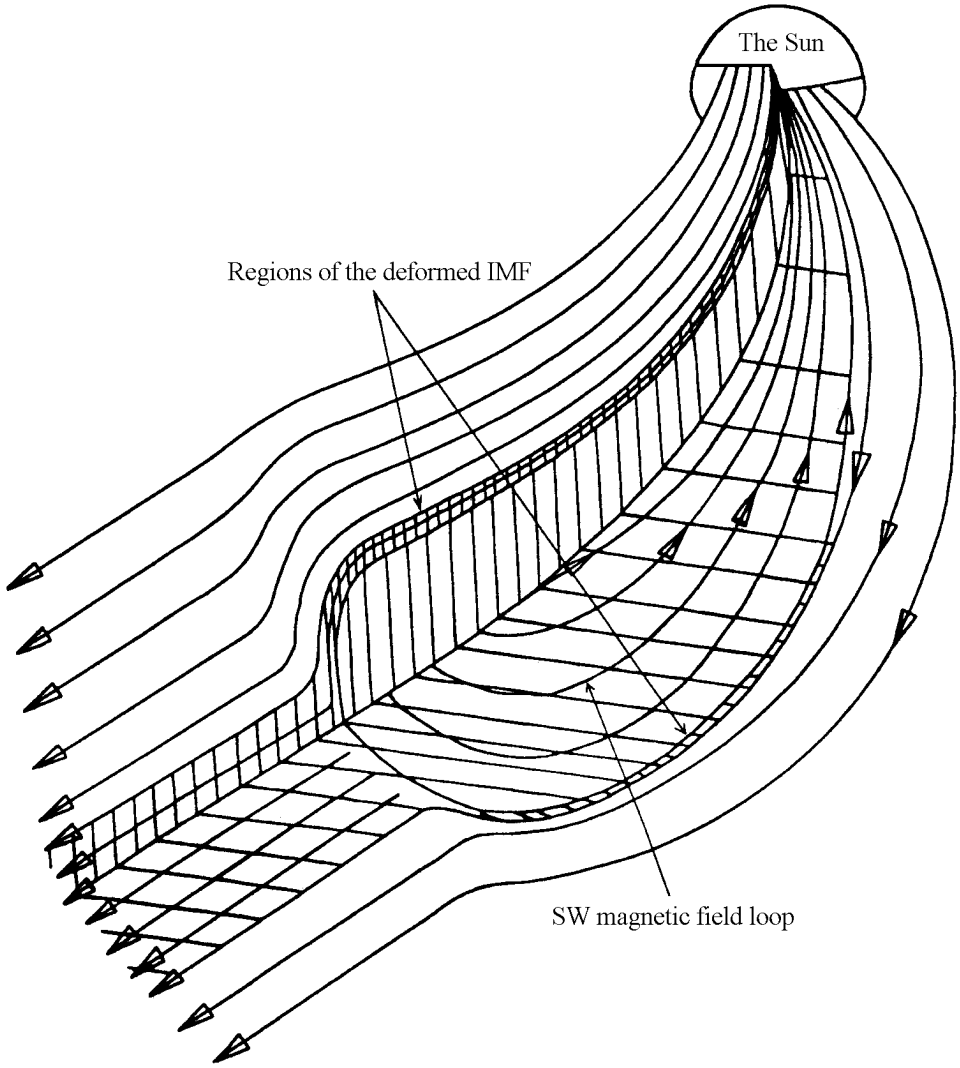

Figure 5. Hypothetical geometry of a high-velocity flux magnetic field that allows one to explain the IMF data in combination with the results of the observation analysis.

tions for the generation of $E_{\rm pl}$. In loop-like structures, a particle is accelerated up to rigidities R_0, at which the Larmor radius of particles is comparable with the typical size of the acceleration regions.

If it is assumed that the energy variation of particles with $R > R_0$ in inverse proportion to R, then in the general case, in the presence of the potential, vortical, and polarization components of the electric field, the expression for $\Delta\mathcal{E}$ becomes

$$\Delta\mathcal{E} = \begin{cases} \Delta\mathcal{E}_{pt} + \mathcal{E} - \sqrt{\beta(\mathcal{E}^2 - \varepsilon_0^2) + \mathcal{E}_0^2} \\ +\mathcal{E}(1 - e^{\alpha/2}) & \text{if } R < R_0 \\ \Delta\mathcal{E}_{pt} + (\mathcal{E}(R_0) \\ -\sqrt{\beta(\mathcal{E}^2(R_0) - \varepsilon_0^2) + \mathcal{E}_0^2} \\ +\mathcal{E}(R_0)(1 - e^{\alpha/2}))\frac{R_0}{R}) & \text{if } R > R_0 \end{cases} \tag{21}$$

Thus a particle with the energy $\mathcal{E}$, recorded at the Earth's orbit at time t_i, has had the energy $\mathcal{E}+\Delta\mathcal{E}_i$ outside the heliosphere, and the differential rigidity spectrum of the recorded particles, by Liouville's theorem, will be described by the expression

$$J_i(R) \propto \frac{(\mathcal{E} + \Delta\mathcal{E}_i)^{-\gamma+1}(\mathcal{E}^2 - \varepsilon_0^2)^{3/2}}{\mathcal{E}[(\mathcal{E} + \Delta\mathcal{E}_i)^2 - \varepsilon_0^2]^{3/2}} \tag{22}$$

where γ is the spectral index of galactic cosmic rays $J(R) \propto \mathcal{E}^{-\gamma}$, and the rigidity spectrum of the variation will be represented by

$$\frac{J_i}{J_0}(R) = \left(\frac{\mathcal{E} + \Delta\mathcal{E}_i}{\mathcal{E} + \Delta\mathcal{E}_0}\right)^{-\gamma+1} \left[\frac{(\mathcal{E} + \Delta\mathcal{E}_0)^2 - \varepsilon_0^2}{(\mathcal{E} + \Delta\mathcal{E}_i)^2 - \varepsilon_0^2}\right]^{3/2} \tag{23}$$

where $\Delta\mathcal{E}_0$ is the particle energy variation in background electric fields of the SW.

Figure 6 presents the results of calculations of the rigidity spectrum of the variations $(J_i/J_0)(R)$ by formula (23) in view of (21) for different instants of time when $\Delta\mathcal{E}_{\rm pl} =$

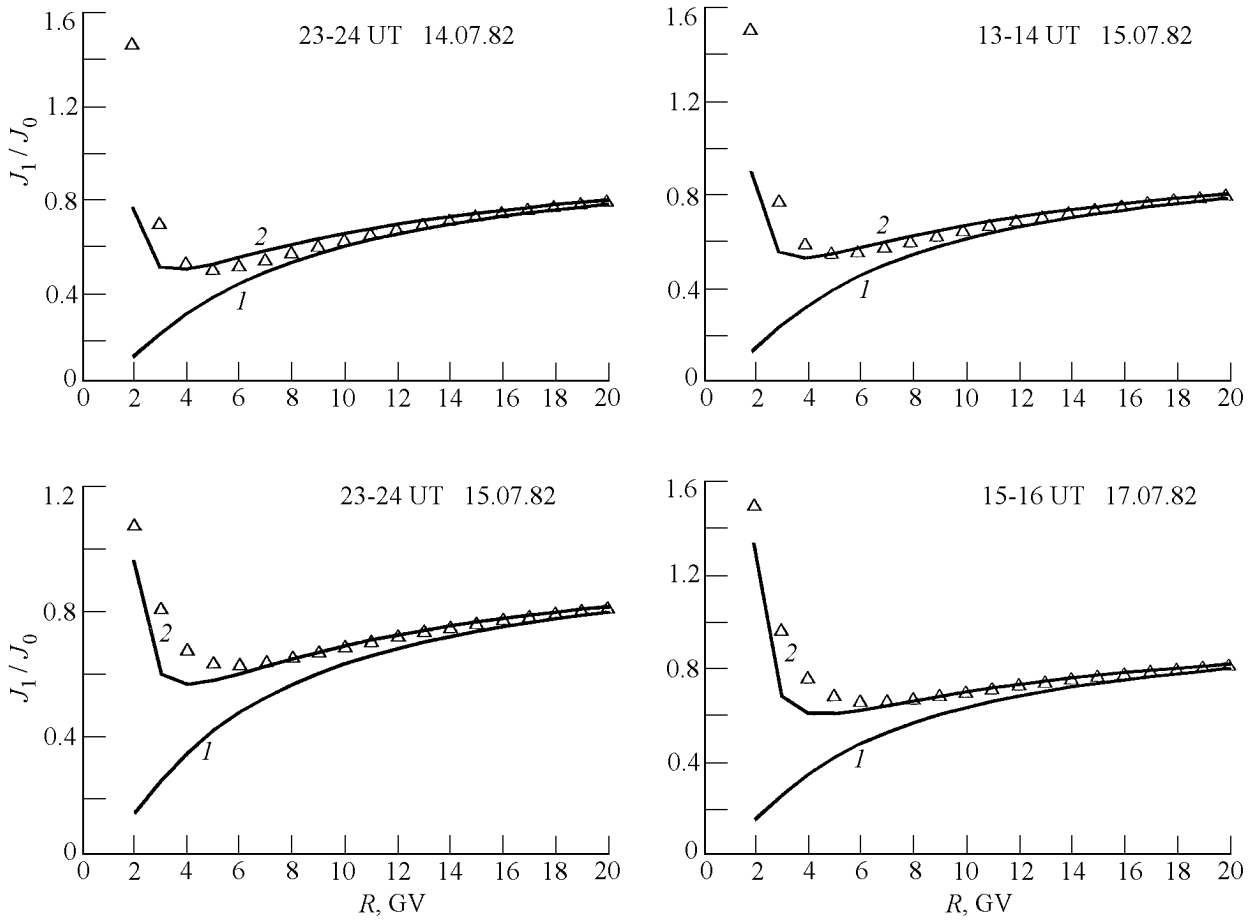

Figure 6. Rigidity spectra of CR variations calculated by formula (23) in view of (21) for the following values of the parameters: $\Delta\mathcal{E}_{pt} = 1.46$, 1.42, 1.31, and 1.31; $\Delta\mathcal{E}_1(R_0 = 1\text{GV}) = -2.25$, -2.33, -2.18, and -2.48; respectively for 2300–2400 UT of 14.07.82, 1300–1400 UT of 15.07.82, 2300–2400 UT of 15.07.82, and 1500–1600 UT of 17.07.82 (curve 2), and for the same values of $\Delta\mathcal{E}_{pt}$, but when $\Delta\mathcal{E}_1 = 0$ (curve 1). Triangles are observed variations of the isotropic component of the CR intensity with respect to the background level on 15 January 1982.

$\Delta\mathcal{E}_{\text{rot}} = 0$ (curve 1) and for nonzero $\Delta\mathcal{E}_{\text{pl}}$ and $\Delta\mathcal{E}_{\text{rot}}$ (curve 2) for the respective values of $\Delta\mathcal{E}_{pt}$. Triangles show the variation spectra obtained by analyzing ground-based observations using the SGS method. The findings indicate that the value of $R_0 \lesssim 2$ GV, hence it is impossible to determine the spectrum parameters α, β, and R_0 using only data from neutron monitors without invoking satellite data. In the rigidity range $R > R_0$, expression (21) has a simplified form

$$\Delta\mathcal{E} = \Delta\mathcal{E}_{pt} + \Delta\mathcal{E}_1 \frac{R_0}{R}$$

where

$$\Delta\mathcal{E}_1 = \mathcal{E}(R_0) - \sqrt{\beta(\mathcal{E}^2(R_0) - \varepsilon_0^2) + \varepsilon_0^2}$$

$$+\mathcal{E}(R_0)(1 - \exp(\alpha/2))$$

In this case, the expression for describing the variation spectrum involves only two unknown parameters $\Delta\mathcal{E}_{pt}$ and $\Delta\mathcal{E}_1 R_0$, which were determined from observed values of $(J_i/J_0)(R)$ (triangles in Figure 6).

As follows from a comparison of observed and calculated values of $(J_i/J_0)(R)$, the observed spectrum can be explained by the superposition of the particle deceleration and acceleration effects along their propagation trajectory from the Galaxy to the point of observation.

Since the energy variation $\Delta\mathcal{E}_1$ in vortical and polarization fields depends on $v_\perp$ and $u_\perp$, the CR intensity variation amplitudes, caused by these variations, must depend on the direction of arrival of the particles at the point of observation, and the anisotropy amplitudes will be determined by the magnitude of the effect from $\Delta\mathcal{E}_1(R_0/R)$ (by the difference between curves 1 and 2 in Figure 6). Furthermore, depending on the particular region of the IMF loop-like structure where an acceleration of particles occurs, either the fundamental or the second spherical harmonics (bidirectional anisotropy) will dominate. If the acceleration occurs due to the polarization component of the electric field

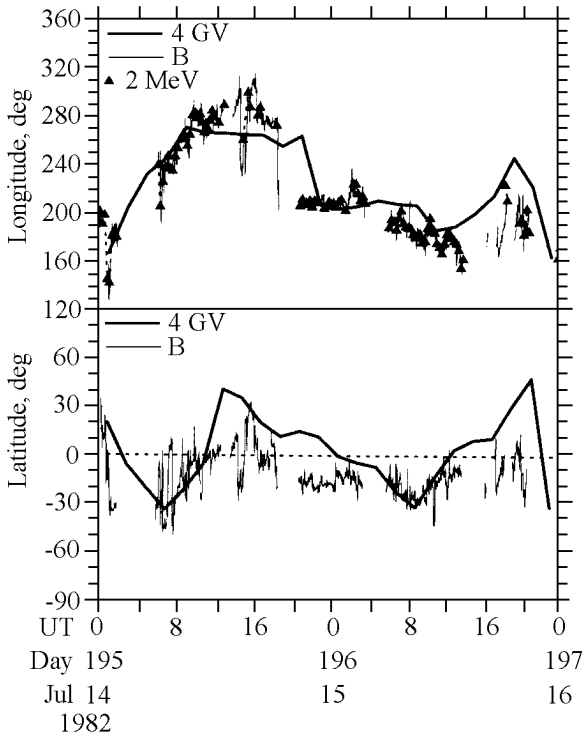

Figure 7. Correlated changes in the direction (top, longitude; bottom, latitude) of the interplanetary magnetic field at ISEE 3 (B; thin line), and second harmonics of the distributions of 4 GV cosmic ray (thick line) and 1–4 MeV ions (triangles), during 14–15 July 1982. The data are consistent with predominately field-aligned bidirectional streaming at 4 GV and 1–4 MeV.

near the point of observation, then the fundamental harmonic will dominate, with the phase orthogonal to the IMF vector (for 1300–1400 UT, for example) on 15 June (see Figure 4). In the case of a particle acceleration at the base of the loop-like structure, a bidirectional anisotropy with a deficiency of particles in large pitch angles can be observed (see right-hand panels in Figure 3). It should be noted that the phase of the CR bidirectional anisotropy can provide information about the IMF orientation. For comparison, Figure 7 (taken from a paper [*Richardson et al.*, 2000]) presents the data on the IMF orientation determined from the bidirectional anisotropy phase of energetic particles and particles with 4 GV rigidity, as well as the data of in situ measurements of the orientation of the IMF vector.

In addition to providing information about the variations of the CR rigidity spectrum and anisotropy outside the magnetosphere, the method used here makes it also possible to obtain information about variations of the planetary system of geomagnetic cutoff rigidities (see Figures 2 and 3). As is apparent from Figure 2, the time profile of ΔR_c is in good agreement with that of the *Dst* index. In the main phase of the magnetic storm, the value of ΔR_c is $\sim$1.5 GV when $R_c = 4$ GV. The dependence of ΔR_c on R_c, obtained from an analysis in different phases of the magnetic storm (left-hand panels in Figure 3), is in qualitative agreement with results of calculations of $\Delta R_c(R_c)$ in terms of the model of the magnetospheric current distributed across the shell in proportion to the latitude cosine and flowing in a westward direction (see right-hand panels in Figure 3). For a quantitative reconciliation, it seems to be necessary to use a more adequate model of a spatially distributed magnetospheric current system.

The reliability of information obtained can be assessed by the degree of correspondence between the geomagnetic cutoff rigidity variations ΔR_c at $R_c = 4$ GV and the *Dst* index (see Figure 2), and from the correspondence of the observed IMF orientation with that determined from the bidirectional anisotropy phase (see Figures 3 and 7), as well as from values of standard deviations δ of observed variation amplitudes from calculated ones.

Acknowledgment. This work was supported by INTAS grant (INTAS 00-0810).

References

Baisultanova, L. M., et al., Magnetospheric effects in cosmic rays during Forbush decrease, in *Proceedings of the XXth International Conference on Cosmic Rays*, vol. 4, p. 231, Moscow, Russia, 1987.

Baisultanova, L. M., A. V. Belov, R. T. Gushchina, L. I. Dorman, V. N. Ishkov, and V. G. Yanke, A preliminary analysis of the solar cosmic-ray increase on September 29, 1989 using data from neutron monitors, *Izv. Akad. Nauk SSSR Ser. Fiz. (in Russian), 55*(10), 1877, 1991.

Chapman, S. B., Cosmic rays and magnetic storms, *Nature, 140*(3540), 423, 1937.

Dorman, L. I., *Cosmic Rays Variations (in Russian)*, 492 pp., Gostekhizdat, Moscow, 1957.

Dorman, L. I., *Galactic Cosmic Rays Variations (in Russian)*, 214 pp., Moscow State Univ., Moscow, 1975.

Dorman, L. I., and M. I. Tyasto, Effect of the sphere-distributed westward current on geomagnetic cutoff rigidity, *Kosm. Issled. (in Russian)*, 7, 131, 1965.

Dvornikov, V. M., and Yu. G. Matyukhin, Energetic losses of cosmic ray travelling in the solar wind regular magnetic field, *Izv. Akad. Nauk SSSR Ser. Fiz. (in Russian)*, *39*(3), 624, 1976.

Dvornikov, V. M., and V. E. Sdobnov, Modification of the method for spectrographic global survey for studying variations in the planetary system of geomagnetic cutoff rigidities, *Izv. Akad. Nauk SSSR Ser. Fiz. (in Russian)*, *55*(10), 1988, 1991.

Dvornikov, V. M., and V. E. Sdobnov, Analysis of the solar proton event on October 19, 1989, by the method spectrographic global survey, *Geomagn. Aeron. (in Russian), 37*(2), 43, 1997a.

Dvornikov, V. M., and V. E. Sdobnov, Time variations of the cosmic ray distribution function during a solar proton event of September 29, 1989, *J. Geophys. Res., 102*, 24,209, 1997b.

Dvornikov, V. M., V. E. Sdobnov, and A. V. Sergeev, Analysis of cosmic ray pitch angle anisotropy during Forbush effect in June 1972 by the method of spectrographic global survey, in *Proceedings of the 18th International Conference on Cosmic Rays*, vol. 3, p. 249, Bangalor, India, 1983.

Dvornikov, V. M., V. E. Sdobnov, and A. V. Sergeev, Anomalous variations of the cosmic ray energy spectrum during some periods of 1972, in *Proceedings of the XXth International Conference on Cosmic Rays,* vol. 4, p. 91, Moscow, 1987.

Krymskiy, G. F., et al., Cosmic ray distribution and reception vectors of detectors, 1, *Geomagn. Aeron. (in Russian), 6*, 991, 1966.

Lockwood, J. A., and W. R. Webber, Differential response and specific yield functions of cosmic ray neutron monitor, *J. Geophys. Res., 72,* 3395, 1967.

McCracken, K. G., et al., Cosmic ray tables, (Asymptotic directions, variational coefficients and cutoff rigidities), in *IQSY Instruction Manual,* no. 10, p. 104, London, UK, 1965.

Morozov, A. I., and L. S. Soloviev, The motion of charged particles in electromagnetic fields, in *Voprosy Teorii Plazmy (in Russian)*, vol. 2, 177, Gosatomizdat, Moscow, 1963.

Nagashima, K., Three-dimensional cosmic ray anisotropy in interplanetary space, *Rep. Ionos. Space Res. Jpn., 25*(3), 189, 1971.

Parker, E. N., *Interplanetary Dynamical Processes,* Interscience Publishers, John Wiley and Sons, New York, 1963.

Richardson, I. G., et al., Bidirectional particle flows at cosmic ray and lower (∼1 MeV) energies and their association with interplanetary coronal mass ejections/ejecta, *J. Geophys. Res., 105*(6), 12,579, 2000.

Shea, M. A., and D. F. Smart, Possible evidence for a rigidity-dependent release of relativistic protons from the solar corona, *Space Sci. Rev., 32*(1/2), 251, 1982.

Shea, M. A., D. F. Smart, and K. G. McCracken, A study of vertically incident cosmic ray trajectories using sixty-degree simulations of geomagnetic field, *Rep. AFCRL-65-705,* Air Force Cambridge Res. Labs., Bedford, Mass., 1965.

Treiman, S. B., Effect of equatorial ring current on cosmic ray intensity, *Phys. Rev, 89*(1), 130, 1953.

World Data Cent. for Cosmic Rays, in *Cosmic Ray Neutron Database*, Toyokawa, Japan.

Webber, W. R., Some features of the response of neutron monitor to low energy particles incident on the atmosphere, *Can. J. Phys., 10,* 906, 1962.

Webber, W. R., and J. J. Quenby, On the derivation of cosmic ray specific yield functions, *Philos. Mag., 4*(41), 654, 1959.

V. M. Dvornikov and V. E. Sdobnov, Institute of Solar Terrestrial Physics, Irkutsk 664033, Russia. (sdobnov@iszf.irk.ru)

(Received 12 March 2001; accepted 11 November 2001)